Experimental Evaluation of Frequency Regulation from Commercial Building HVAC system

Yashen Lin, Prabir Barooah, Sean Meyn, Timothy Middelkoop

***Abstract*— Automated demand response can be a valuable resource for ancillary services in the power grid. This paper illustrates this value with the first experimental demonstration of frequency regulation from commercial building Heating Ventilation and Air Conditioning (HVAC) systems. The experiments were conducted in a 40,000 sq. ft. commercial building located at the University of Florida campus. Detailed are the steps required to make this possible, including control architecture, system identification, and control design. Experiments demonstrate: 1. Satisfactory frequency regulation service can be provided by the HVAC system without noticeable effect on the indoor climate, and 2. The ancillary service provided by this system passes the qualification criteria for participating in PJM Interconnection's frequency regulation market.**

I. Introduction

Ancillary services are needed to correct the mismatch between demand and supply in a power grid. As more renewable energy sources are introduced into a power grid, the volatility of supply also increases, resulting in the need for additional ancillary services [1].

Ancillary services can be broadly divided into two categories: (i) those used continuously during normal operation; (ii) those used in contingency situations, such as following the loss of a generator. This paper focuses on frequency regulation, which falls in the first category. Frequency regulation corrects the short-term imbalance in the grid, usually on time scales of seconds to minutes [2]. The need for this service is well recognized based on engineering considerations, and consequently this is one of the ancillary services with a well developed market to incentivize service [3]. The Federal Energy Regulatory Commission (FERC) has recognized the need for increasing ancillary services through several new rulings, such as the recent FERC order 755 [4] that demands payment for ancillary services in higher frequency bands.

Traditionally, frequency regulation has been provided by responsive power generators, which has several drawbacks. Generators must withhold power to provide these ramping services, there is additional cost to generators in terms of both fuel and maintenance. Ramping of generation output also has cost in the form of additional pollution [5]. Finally, it is costly to build new generators to satisfy the increasing demand for ancillary services.

YL and PB are with the MAE dept. and SM is with the ECE dept. at the University of Florida; yashenlin,pbarooah@ufl.edu,meyn@ece.ufl.edu. TM is with the University of Missouri; MiddelkoopT@missouri.edu.

This research is supported by the NSF grants CPS-0931416 & ECCS-0925534, and DOE awards DE-OE0000097 & DE-SC0003879.

Recent research have shown that the demand side is capable of providing abundant high quality ancillary services, see for example [3], [6]–[9]. Buildings are a tremendous untapped resource for several reasons. First, they are large energy consumers, accounting for 74% of total electricity consumption in the U.S. [10]. Residential loads, such as A/C and refrigerators, can be aggregated to provide ancillary service; see for example [6], [9], [11], [12]. Manufacturing companies such as Alcoa Inc provide demand side ancillary services today on a range of time scales [13].

We believe that HVAC system in commercial buildings provide significant potential value that can be harnessed easily. Consumption of energy is very flexible, in part because of the thermal inertia in large buildings. Most commercial building HVAC systems have continuous control variables, which provides flexibility in control design compared to on-off control commonly used in residential buildings. Commercial buildings are usually equipped with Building Automation System (BAS), which simplifies the installation of new control algorithms. These features also makes it possible to provide ancillary service without aggregation of a large number of buildings.

Simulations presented in [7] show that continuous adjustment of the supply air fan in the Air Handling Unit (AHU) in a commercial building can be used to provide frequency regulation in the frequency range of $f \in [1/(3\text{ min})\ ,\ 1/(8\text{ sec})]$, with negligible impact on room climate. An indirect approach proposed in [14], argues that ancillary service can be obtained by modulating the supply duct static pressure, which changes the power delivered to the supply-air fan. If the chillers in the HVAC system are included, then the frequency range of ancillary service can be extended to low frequencies, down to $1/(1\text{ hour})$ [8].

All of this previous work was based on theory and simulations. To the best of our knowledge, this paper is the first to report implementation of HVAC control in a real building to provide frequency regulation.

The experiments reported here demonstrate that a building HVAC system can provide frequency regulation service without affecting its primary responsibility — maintaining comfortable indoor climate. This work is inspired by our prior, simulation-based, studies on using HVAC fans to provide frequency regulation. The control architectures used here are, however, quite distinct from those in [7], [15], [16]. We demonstrate two distinct feedback control architectures to extract ancillary service by varying fan power consumption. In one, the fan speed is commanded directly, while in the other it is varied indirectly through changing the flow-rate setpoint.

Each control design is based on black-box transfer functions obtained through system identification.

The control algorithms are tested with filtered regulation signals obtained from PJM: The Area Control Error (ACE) signal as well as the dynamic regulation signal (RegD). Results show that the controllers introduced here have satisfactory performance in the frequency range of $f \in [1/(10\text{ min})\ ,\ 1/(30\text{ sec})]$, and will pass the PJM qualifying test [17].

Based on these experimental results, we estimate the economic value of building used in these experiments if it were to take part in PJM's ancillary service market, and the total amount of ancillary service that similar commercial buildings in the U.S. can provide through software retrofit.

II. Problem Formulation

The control architecture described in this section is a software add-on for an existing HVAC control system. We first briefly review typical HVAC systems before describing this control architecture.

A. Typical HVAC system in a commercial building

Fig. 1 shows the schematic of a Variable Air Volume (VAV) HVAC system; 30% of U.S. commercial building floorspace is serviced by such systems [18]. A part of return air is mixed with outdoor air, which is cooled and dehumidified while it passes through the cooling coil in the AHU. The air is distributed to terminal devices, called VAV boxes, through ducts for distribution into individual zones. A supply air fan motor in the AHU provides the mechanical energy required to circulate the air.

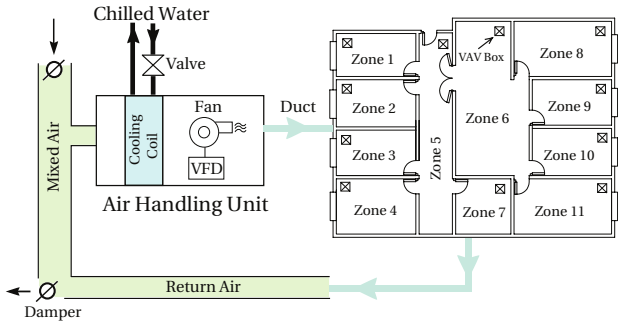

Fig. 1. Typical commercial building VAV HVAC system.

Highlighted in Fig. 2 are a few of many control loops in a HVAC system. The fan control loop and zone climate control loop are emphasized since they will be a focus of this paper. The zone climate controller compares the measured zone temperature T to a predetermined setpoint T_{ref} to compute a desired supply air flow rate m_{ref} to achieve the desired zone climate. The fan controller computes the fan command u_f to ensure that the supply air flow rate m_a tracks m_{ref}. In a VAV system, the fan motor speed is varied through a Variable Speed Drive (VSD), so the command u_f is sent to the VSD. The fan

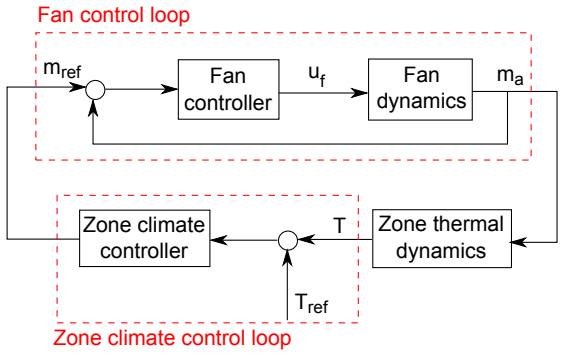

Fig. 2. Control loops in the AHU relevant to this paper. The zone climate control loop determines the desired supply air flow rate to maintain room temperature; the fan control loop commands the fan to produce that flow rate.

command u_f is measured in the unit of % of the maximum speed.

B. Proposed control architecture

The goal of the control architecture described here is to provide ancillary service to the grid while ensuring that its actions have little effect on the indoor climate. In this paper we assume that a resource that provides frequency regulation service receives a signal from a Balancing Authority (BA), denoted by δP_{BA}, which is then filtered with a bandpass filter to generate a local reference signal, δP_r. Fig. 3 illustrates the proposed control architecture. The resource's responsibility is to vary its power generation/consumption so that the deviation from its baseline power profile tracks the reference signal δP_r. The baseline power is the power the resource would have consumed had it not been involved in providing ancillary service.

The local reference signal δP_r is both scaled and filtered. In some cases, BA broadcasts filtered version of the ACE and δP_{BA} is already of suitable frequency. The band-pass filter in Fig. 3 then becomes a scalar gain to obtain appropriate magnitude. This will be the case when we take PJM's RegD signal as a reference δP_{BA}.

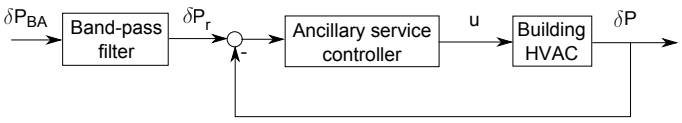

Fig. 3. Proposed control architecture of building HVAC system providing ancillary service.

The passband of the bandpass filter and its passband gain will vary from building to building, depending on the capacity of its HVAC equipment, its thermal inertia, etc. In this paper we assume that each building is free to design its own bandpass filter to ensure that its equipment is not damaged and its indoor climate is not adversely affected by the ancillary service it provides.

The design problem considered in this paper involves the "Ancillary Service Controller", which is local to the building system. This controller addresses a reference tracking problem: commands to the AHU fan are modified in real-time so that

δP, the measured deviation from the baseline power, tracks the reference deviation δP_r. Algorithms to estimate the deviation from baseline in real-time are described at the end of this section.

The control signal u in Fig. 3 could be any command that changes the fan motor's power consumption. In this paper, we will explore two options, indicated as u_1 and u_2 in Fig. 4.

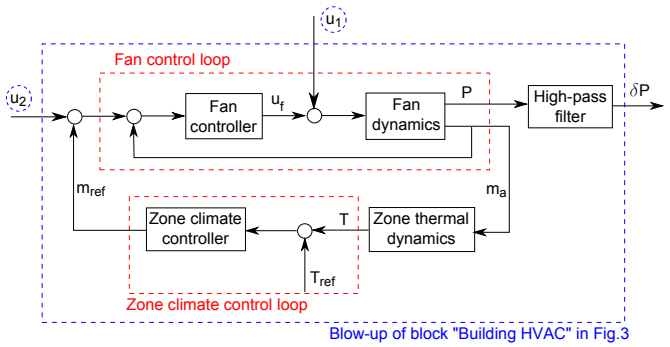

Fig. 4. Two locations to inject control command in the local control loop.

Utilization of the input u_1 is adopted from [7]: the Ancillary Service Controller simply modifies the fan speed command u_f. In effect, the control command enters the existing HVAC control system as a disturbance (ignoring the feedback effect). The motivation comes from the fact that since the fan motor has fast dynamics, it can react quickly to track a high frequency reference signal. Low frequency variations of u_1 are not effective, since the local fan controller will reject the ancillary service control command as a disturbance [7].

The second option u_2 is a deviation to the baseline supply air flow rate m_{ref}. A change in the flow rate will result in a change in the fan motor power consumption. The zone climate control loop is usually less aggressive than the fan control loop, and is therefore unlikely to reject the low-frequency "disturbance" u_2. The second option is a complement to the use of u_1 since it is difficult to obtain high frequency ancillary service using u_2.

In the experiments reported here, we vary the air flow rate by commanding the flow rate setpoint. In AHUs where the air flow rate is controlled indirectly through static presssure setpoint, control can be executed by varying the static presssure setpoint.

We will call the first option ASHFS (Ancillary Service controller for High frequency reference signal through Fan Speed command), and the second option ASLAF (Ancillary Service controller for Low frequency reference signal through Air Flow setpoint).

The Ancillary Service Controller described here does not override the existing HVAC control system, it merely modifies the commands in the HVAC system. A key requirement in choosing the control inputs is ease of implementation. Both the fan speed command and airflow rate setpoints can be modified through software in AHU2 of Pugh Hall that was used as our testbed. In AHUs where the air flow rate is controlled by static pressure, there is usually a static pressure setpoint, so that u_2 could be a command added to this setpoint.

The deviation δP is not directly measured; instead only the power measurement P is available from the VSD. To obtain δP, we take advantage of the fact that reference signal has higher frequency than the dynamics of building HVAC system. The baseline power can be estimated on-line by passing P through a low-pass filter. The deviation from baseline, δP, can then be estimated by subtracting the estimated baseline from P. This is equivalent to using a high-pass filter; see Fig. 4. We denote this estimated power deviation by $\delta \hat{P}$.

III. System Identification

Design and analysis of the Ancillary Service Controller requires a model of how the command u affects fan power. In our earlier studies [7], [8], each component in the HVAC system is modeled and integrated to form the full model. However, dynamics of HVAC systems are highly uncertain and information about some of the local control loops is hard to obtain. Fortunately, information about all the components is not necessary for controller design. In this section we describe how an input-output model was fit to data obtained at our test bed.

It is known that a physics-based model for HVAC system dynamics is nonlinear. For the purposes of control, it is found that a linear input-output model can be fit to data within the frequency range of interest. The input of the system is the variation in u from its baseline value. Since there in no Ancillary Service Controller during normal operation, the input is simply u. The output of the system is the power deviation from its baseline power profile δP. Since we consider two different inputs, u_1 and u_2, we will identify two input-output models: u_1 to δP, which we will call H_1, and u_2 to δP, which we will call H_2.

A. Test bed

The field experiments are carried out in Pugh Hall on the University of Florida campus. It has a floor space of 40,000 ft^2, a VAV HVAC system, and 3 AHUs. We choose AHU2 for this test which is dedicated to a single auditorium. Fig. 5 shows data from a 24-hour period during normal operation collected from AHU2 of Pugh Hall.

The building is equipped with a Siemens' APOGEE™ BAS. The software system samples all the building "points" (sensor/actuator/setpoint values) and makes them available for real-time control and off-line analysis. In particular, the fan speed command u_f and supply air flow rate setpoint m_{ref} can be set through PPCL code [19], and new control logic can also be coded into the BAS via PPCL code.

In the tests reported in this paper, we utilized a custom control system software instead of modifying PPCL programs. Partial details of the software are described in [20].

Due to the massive data volumes involved, data collection occurs on change-of-value (COV) events to avoid spikes in network traffic. The control software is designed to simultaneously support a number of applications by interacting with various databases. Control commands from the applications

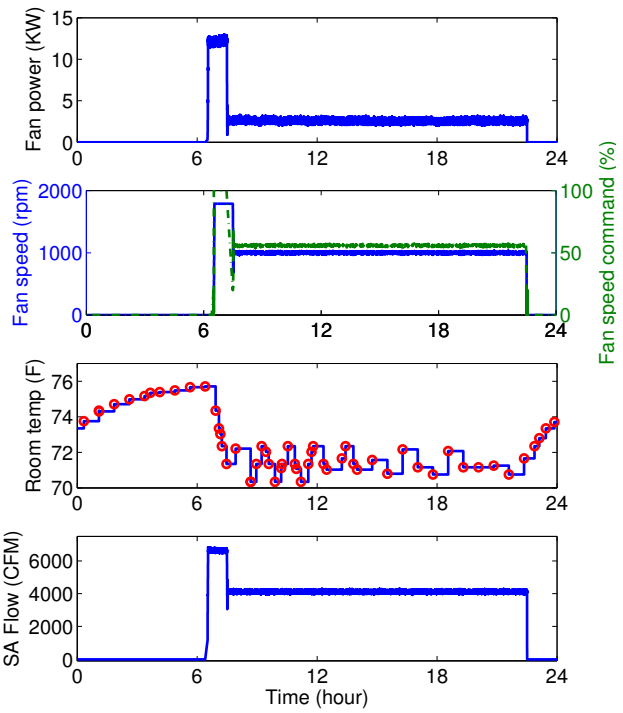

Fig. 5. Data from a typical day during normal operation from AHU2 in Pugh Hall. The AHU is shut down from 11 p.m. to 6 a.m. as part of a "night time set back" strategy for reducing energy use.

are communicated to the system by appending a row to a table in a relational database. A scheduler, which checks for such updates every second, then communicates these new commands to the equipment controllers through BACnet [21]. In our experiments, inputs were commanded at 4 second intervals and outputs were averaged and/or interpolated to generate values sampled at 4 second intervals.

Measurement noise: It was found that measurement noise is not negligible. Fig. 6 shows power measurements obtained over 10 minutes while the fan speed control command was set to a constant value of 55%. Also shown is an estimate of the power spectral density, which is consistent with white noise. The final plot in this figure is an estimate of the *marginal distribution* of the measurement noise, based on a histogram of observations.

B. Sine-sweep experiments

Frequency domain identification is preferable to fitting a parameterized linear model because of strict constraints on the magnitude of the inputs. Due to the large measurement noise, the sine-sweep method was used for estimating the frequency response [22].

Sine-sweep tests were conducted by modifying the fan speed (or mass flow rate setpoint) command through the control software in such a way that u_1 (u_2) becomes a sinusoidal signal with given frequency. In these experiments the nominal fan power was equal to 2.5kW, and for each frequency, the number of data points collected was approximately 500.

We describe first the identification of the transfer function from u_1 to δP, denoted by H_1. The frequency response estimates obtained from the experiment are shown

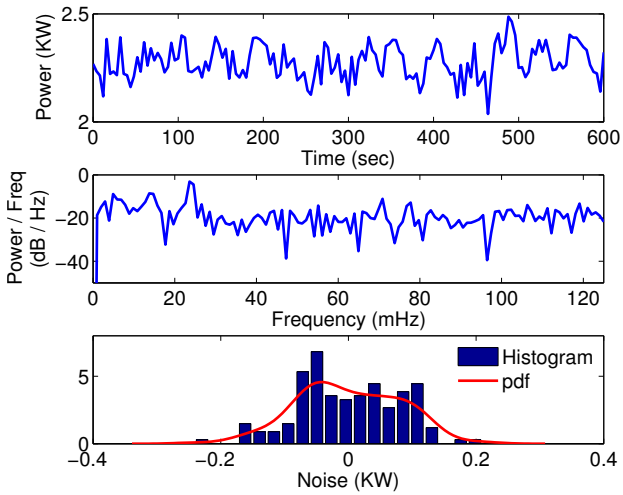

Fig. 6. Measurement noise characterization. Top: time domain power measurement; middle: power spectrum density of the noise; bottom: histogram and fitted probability density function of the marginal distribution.

in Fig. 7. The magnitude plot peaks between the frequency $f \in [1/(1\text{ min}),\ 1/(30\text{ sec})]$. For lower frequency, the input is rejected by the local controller; for higher frequency, the response decays due to the dynamics of the fan and motor. A "best-fit" linear model obtained from this experiment has second-order transfer function,

$$\hat{H}_1(s) = \frac{0.0173s + 1.7280 \times 10^{-6}}{s^2 + 0.0360s + 0.0144} \tag{1}$$

Its frequency response is shown on the left hand side of Fig. 7.

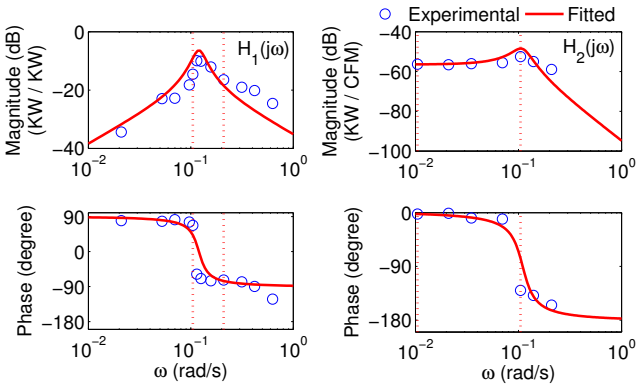

Fig. 7. Frequency response of H_1 (left) and H_2 (right) identified from sine-sweep experiments, as well as the Bode plots of the fitted transfer functions.

Similarly, sine-sweep experiments using input u_2 were conducted to obtain frequency response data used for identifying the system from u_2 to δP, denoted by H_2. The fitted transfer function is,

$$\hat{H}_2(s) = \frac{1.809 \times 10^{-5}}{s^2 + 0.04455s + 0.01205}, \tag{2}$$

The results of these experiments are summarized in the plots shown in Fig. 7. The frequency response shows that the system has a nearly constant gain in the range $f \in$

$[1/(10\text{ min})\ ,\ 1/(1\text{ min})]$, which simplifies control design to track reference in this frequency range.

IV. Controller design and simulation

The details of the controller design and simulation study are summarized in this section.

Recall that the feedback architecture for Ancillary Service Controller is illustrated in Fig. 3. The goal is to provide regulation service to the grid, while respecting indoor climate constraints. To ensure the latter, large variation in the fan speed or air flow rate is to be avoided. Such variations are undesirable also due to the possibility of equipment damage and violation of indoor air quality standards [23]. In addition, the fan speed command is subject to magnitude constraints, since it takes values between 0 and 100%.

For these reasons, the frequency ranges for providing ancillary service are chosen where the system has large gain. Considering the frequency response identified in Section III leads to $f \in [1/(1\text{ min})\ ,\ 1/(30\text{ sec})]$ for ASHFS and $f \in [1/(10\text{ min})\ ,\ 1/(1\text{ min})]$ for ASLAF.

We do not attempt to track reference signals of frequency lower than $1/(10\text{ min})$. The reason is that if the fan speed or air flow rate is increased or reduced for long time periods, power consumption at the chiller will be affected; while variations in fan speed or air flow rate at higher frequency ranges will be "filtered out" by the low-pass characteristics of the chiller, and hence do not impact power consumption at the chiller [8].

A. ASHFS

The band of frequencies in which the controller is required to perform reference tracking is narrow, $f \in [1/(1\text{ min})\ ,\ 1/(30\text{ sec})]$, and the passband of the transfer function H_1 is very narrow. Hence a proportional controller was found to be adequate for ASHFS.

Recalling that $H_1(j\omega)$ denotes the open-loop frequency response obtained from the sine-sweep experiments, the closed-loop frequency response using proportional control with gain k_p is given by:

$$H_1^{ry}(j\omega) = \frac{k_p H_1(j\omega)}{1 + k_p H_1(j\omega)} \tag{3}$$

The frequency response from the reference signal to the control command determines the amount of actuation required. This is given by,

$$H_1^{ru}(j\omega) = \frac{k_p}{1 + k_p H_(j\omega)} \tag{4}$$

It was assumed that for a reference signal with peak magnitude 1kW, the fan speed can be varied within 10% of its nominal value. This is equivalent to $|H_1^{ru}(j\omega)| \leq -20dB$ in the range where frequency regulation will be provided.

The proportional gain k_p was tuned so that (i) $H_1^{ry}(j\omega)$ is close to 1 in the frequencies of interest for good tracking performance; (ii) $|H_1^{ry}(j\omega)|$ is small outside that range for noise and disturbance rejection; (iii) $|H_1^{ru}(j\omega)|$ is not too large in the frequency of interest to avoid actuator saturation. The proportional gain $k_p = 15$ meets these criteria. The closed loop frequency response is shown on the left in Fig. 8.

B. ASLAF

Because of the broader passband in the transfer function H_2, and for the benefit of noise attenuation, a lag compensator was chosen,

$$C_{lag}(s) = k\frac{s - z}{s - p} \tag{5}$$

in which $z > p$. With the pole set to $p = -0.0017$, the zero set to $z = -0.6283$, and gain set to $k = 30$, it was found that good tracking performance was obtained with small actuation.

The frequency response of the closed-loop system, $H_2^{ry}(s)$, is shown in Fig. 8. Tracking is reasonable (the gain is nearly unity) in the frequency range of interest, $f \in [1/(10\text{ min})\ ,\ 1/(1\text{ min})]$.

For a reference signal of peak magnitude 1kW, it is assumed that the supply air flow rate can vary within $1000CFM$ of its nominal value. This is equivalent to $|H_2^{ru}(j\omega)| \leq 60dB$, which is also met in the frequency range of interest.

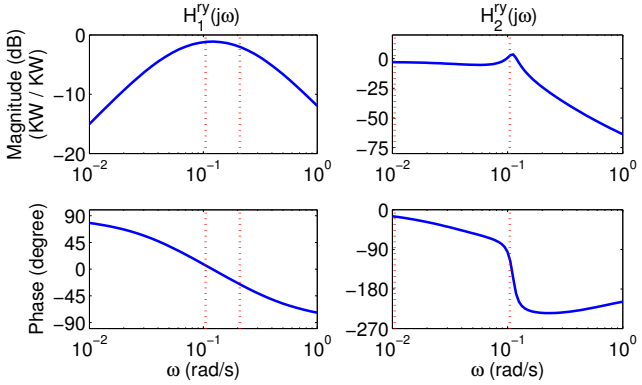

Fig. 8. Closed-loop frequency response from reference to output. The dashed vertical lines indicate the frequency range in which frequency regulation is provided.

C. Performance Criteria

The dual goals of the Ancillary Service Controller are frequency regulation to the grid, while maintaining indoor climate quality as well as low cost to the building operator. Metrics to quantify performance are described here.

Frequency regulation: A natural metric to quantify the quality of tracking error $e(i) := \delta P_r(i) - \delta\hat{P}(i)$ is the ratio,

$$r_R = \frac{E_R}{\max|\delta P_r|} \tag{6}$$

in which the numerator is the root mean square (RMS) value: $E_R = \sqrt{\frac{1}{N}\sum_{i=1}^{N} e(i)^2}$, and the denominator is the maximum of the power deviation signal.

In addition to r_R, we also evaluate the Ancillary Service Controller using PJM's performance score, based on the formula given in their manual [17]. The total performance score S_t is the mean of three scores: correlation score S_c, delay score S_d, and precision score S_p. A score of $S_t \geq 0.75$ is required to pass the PJM test.

Indoor climate: Indoor climate quality was quantified using the temperature violation D_T defined in [24]. This score is based on the minimum and maximum temperature allowed when the building is occupied, set to $70^\circ F$ and $75^\circ F$ according to the thermal comfort specifications described in [25, Chapter 8].

Variation in supply air flow rate comes with some cost. This variation is quantified by,

$$\delta m_{a,avg} = \frac{1}{N}\sum_{i=1}^{N}\left|\frac{m_a(i)-m_b(i)}{m_b(i)}\right| \quad (7)$$

$$\delta m_{a,max} = \max\left|\frac{m_a(i)-m_b(i)}{m_b(i)}\right| \quad (8)$$

where m_a is the measured supply air flow rate, and m_b is the baseline supply air flow rate.

D. Simulation

Reference signals: Three types of reference signal δP_r are used in this paper. Two of them are obtained by passing the ACE signal through a bandpass filter, in which the raw ACE data was from PJM on the day 05/04/2009. As discussed in Section IV, the band-width are chosen to be $f \in [1/(1\text{ min}),\ 1/(30\text{ sec})]$ for ASHFS and $f \in [1/(10\text{ min}),\ 1/(1\text{ min})]$ for ASLAF. A fifth-order Butterworth filter was used to obtain δP_r in this frequency range. In the sequel, we will call the first one Fast ACE, and the second Slow ACE. The other type of reference signal is RegD, which is broadcast by PJM to frequency regulation participants. Its magnitude is between -1 and 1.

Simulation results: Prior to testing on an actual building, simulations were conducted using the identified models $\hat{H}_1$ and $\hat{H}_2$. Based on the discussion in Section III-A, a stochastic model was used in which the measurement noise was white and Gaussian, with standard deviation $\sigma = 0.1$.

The ASHFS was tested using the Fast ACE signal, and the ASLAF was tested with Slow ACE and RegD. The reference signals and the resulting power deviations with the two controllers are shown in Fig. 9 and 10. The resulting performance metrics are shown in Table I. The PJM performance score S_t are above the required threshold 0.75 in all experiments, which indicates satisfactory performance. In simulation, the true power deviation without the measurement noise is also available. The performance metrics recalculated with the true values are also shown in Table I.

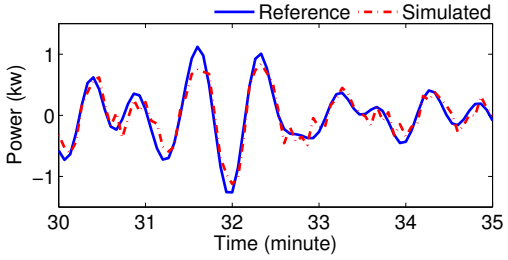

Fig. 9. Simulation result of ASHFS: a 5-minute slice of reference signal and simulated power deviation.

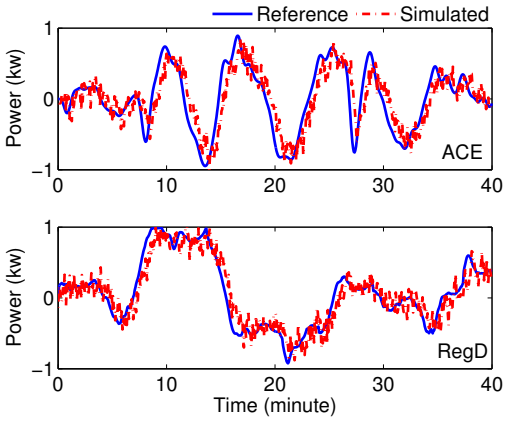

Fig. 10. Simulation result of ASLAF with lag compensator. Top: filtered ACE as reference signal; bottom: RegD as reference signal.

TABLE I

PERFORMANCE METRICS IN SIMULATION.

Simulation	Reference	S_t	r_R
ASHFS	Fast ACE	0.86	0.18
ASHFS (True output)	Fast ACE	0.89	0.15
ASLAF	Slow ACE	0.79	0.25
ASLAF (True output)	Slow ACE	0.82	0.22
ASLAF	RegD	0.85	0.18
ASLAF (True output)	RegD	0.88	0.15

V. EXPERIMENTAL RESULTS

Each experiment was conducted over a 40 minutes time duration using AHU2 at Pugh Hall. Forty minutes is equal to the length of the test required by PJM to meet their qualification criteria [17]. Findings from experiments surveyed here were consistent with simulation experiments, though performance sometimes degraded slightly in building tests.

In our previous study [7], estimates based on a calibrated model of the AHUs at Pugh Hall implied that 11kW of ancillary service capacity could be provided by this building. The experiments reported here show that Pugh Hall's AHUs provide a little less — at 8.7kW, under the operating conditions at the time of these experiments. Consequently, the total frequency regulation potential of U.S. commercial buildings with VAV systems is also slightly less than that claimed in [7].

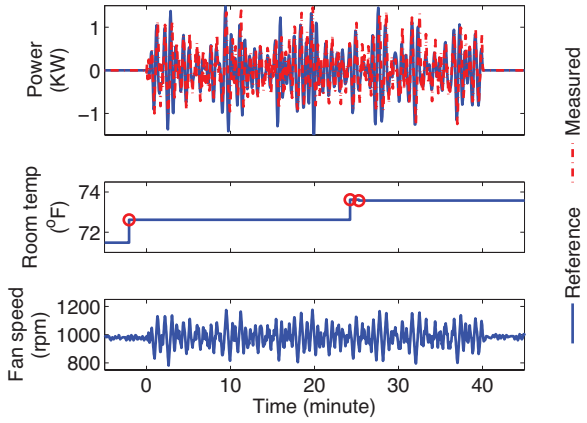

Fig. 11. Experimental results of the ASHFS controller test in AHU2 of Pugh Hall.

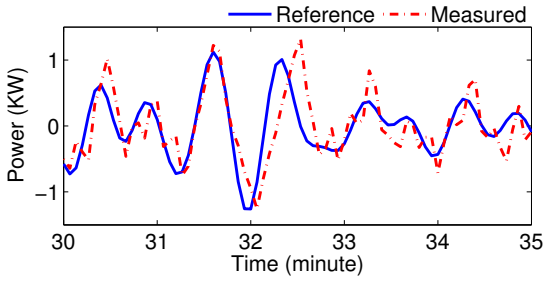

Fig. 12. A 5-minutes slice of the data (reference and output) from the ASHFS experiment.

A. ASHFS experiments

To test the ASHFS, we use the Fast ACE signal described in Section IV-D. The tracking performance, room temperature variation, and supply air flow rate during the test are shown in Fig. 11. A five-minute closeup of tracking performance is also shown in Fig. 12.

The PJM score 0.74 taken from Table II is marginally lower than the threshold 0.75. This score is lower than that in the simulation, which is not unreasonable because the estimated model $\hat{H}_1$ is not a very accurate description of the real system.

The variation in room temperature is small, with $D_T = 0$, meaning there was no temperature violation. The variation in supply air flow rate can be calculated by subtracting the estimated baseline value from the measured data. As shown in Table III, the average variation is less than 4% and the maximum variation is less than 20%.

B. ASLAF experiments

The experimental setup again followed the simulation setup described in Section IV-D, using the same lag compensator, and using the Slow ACE and RegD signals. Data from two typical runs are shown in Fig. 13.

Despite noise and uncertainties in the real building, the experimental data showed very good match with the simulation results.

The control system's scores summarized in Table II exceeded PJM's threshold in both cases. Table III summarizes building performance: The effect on room climate is negligible, the average variation $\delta m_{a,avg}$ is less than 4%, and the maximum variation $\delta m_{a,max}$ is less than 15%.

TABLE II

PERFORMANCE METRICS FOR EXPERIMENTS.

Test	Reference	r_R	PJM performance score			
			S_c	S_d	S_p	S_t
ASHFS	Fast ACE	0.30	0.80	1	0.41	0.74
ASLAF	Slow ACE	0.27	0.94	0.94	0.44	0.77
ASLAF	RegD	0.19	0.94	0.95	0.60	0.83

TABLE III

EFFECTS OF ANCILLARY SERVICE CONTROLLER ON ROOM CLIMATE.

Test	Reference	D_T	$\delta m_{a,avg}$ (%)	$\delta m_{a,max}$ (%)
ASHFS	Fast ACE	0	3.4	17.1
ASLAF	Slow ACE	0	3.4	13.8
ASLAF	RegD	0	3.9	15.0

C. Estimation of frequency regulation

The PJM scores might be better than reported above since measurement noise is included in the computation of $\{S_c,\ S_d,\ S_p,\ S_t\}$.

To improve the estimate of power deviation we passed the measurements through a bi-directional low-pass filter. The filter used is a 5^{th} order Butterworth filter with cutoff frequency at $1/(30\text{ sec})$ for RAFS experiments and $1/(60\text{ sec})$ for ASLAF experiences. Recalculated with this filtered power deviation, performance scores improved; see Table IV. In particular, all of them exceed PJM's 0.75 requirement.

TABLE IV

PERFORMANCE METRICS WITH FILTERED MEASUREMENTS.

Test	Reference	r_R	PJM performance score			
			S_c	S_d	S_p	S_t
ASHFS	Fast ACE	0.27	0.83	1	0.49	0.77
ASLAF	Slow ACE	0.24	0.98	0.94	0.50	0.81
ASLAF	RegD	0.14	0.99	0.94	0.73	0.89

D. Economic potential

What is the economic value of Pugh Hall or similar buildings to a BA? An estimate of the revenue that can be obtained from PJM can be computed based on their publicly available policy manuals [26], [27].

In the Pugh Hall experiments, AHU2 was operating at 2.5kW. Results show that AHU2 can easily provide 1kW capacity of frequency regulation during its operational hours: 6 am to 11 pm. There are two other AHUs which normally operates at 7kW and 5kW. At this operating condition, Pugh Hall's HVAC system can provide 8.7kW of capacity. Time-varying market data was obtained in 2013 from the PJM website [28]. Assuming that the building provides 8.7 kW of capacity of RegD service during each of its operational hours, the yearly revenue for Pugh Hall is estimated to be $\$2,135$. The total capacity of the AHUs are much higher than the operating point used in the calculation, and more revenue can be generated if they operates at higher power.

VI. DISCUSSIONS AND FUTURE WORK

HVAC systems in commercial buildings can provide frequency regulation service to the power grid without adversely impacting indoor climate. This has been demonstrated in this paper using two feedback control architectures, designed to provide ancillary service in a specific frequency range.

Experimental results at Pugh Hall at the University of Florida show that these algorithms pass the qualifying tests to participate in PJM's frequency regulation service market. This single building would generate approximately $2,000 revenue per year based on PJM's 2013 prices.

There are many directions for future research:

1) There are many other loads in a building, such as chillers and variable speed pumps. A control architecture for harnessing ancillary service from commercial building chiller, and a collection of residential pool pumps, have

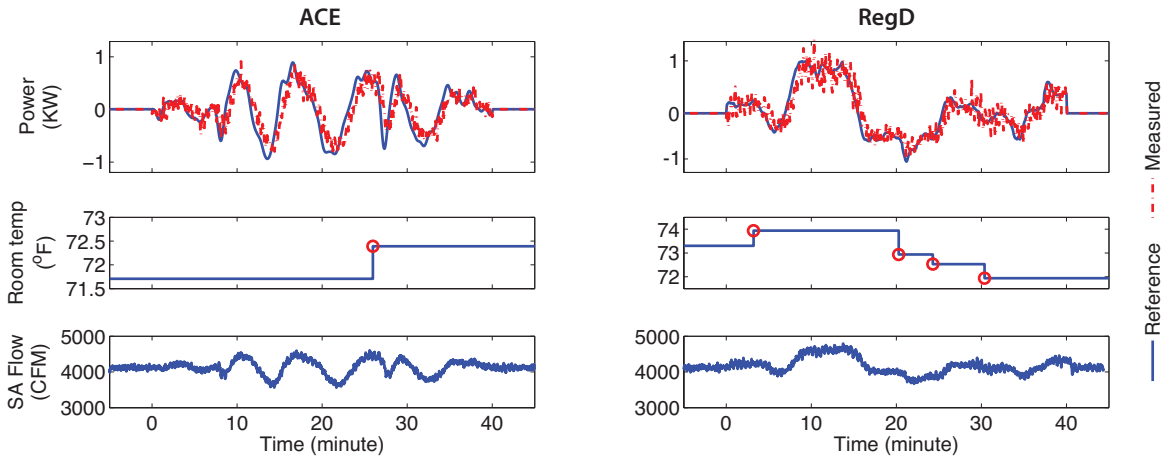

Fig. 13. Experimental results for ASLAF with lag compensator. Left: with filtered ACE as reference signal; right: with RegD as reference signal.

been presented in [8] and [9], respectively. Further work will investigate the impact of harnessing several different loads for ancillary service simultaneously.

2) The control architecture proposed in this paper is a software add-on. Improvements in hardware and software can lead to better performance (e.g., improving measurement accuracy and reducing execution delay).
3) Further thoughts on information architecture should be considered in future work. For example, it may be useful to base control actions based on local frequency deviations in the power lines along with a global signal broadcast from the balancing authority.

ACKNOWLEDGMENTS

The authors thank personnel at the Physical Plants Division at the University of Florida, in particular Peder Winkel, for their help in conducting the field tests in Pugh Hall.

REFERENCES

[1] S. Meyn, M. Negrete-Pincetic, G. Wang, A. Kowli, and E. Shafieepoorfard, "The value of volatile resources in electricity markets," in *Decision and Control (CDC), 2010 49th IEEE Conference on*. IEEE, 2010, pp. 1029–1036.

[2] B. Kirby, "Ancillary services: technical and commercial insights," 2007. [Online]. Available: http://www.science.smith.edu/~jcardell/Courses/EGR325/Readings/Ancillary_Services_Kirby.pdf

[3] J. MacDonald, P. Cappers, D. Callaway, and S. Kiliccote, "Demand response providing ancillary services," *Grid-Interop*, 2012.

[4] Federal Energy Regulatory Commission, "Order No.755 Frequency Regulation Compensation in the Wholesale Power Markets: Comments of ISO/RTO Council," May 2011.

[5] D. Lew, G. Brinkman, E. Ibanez, B. Hodge, and J. King, "The western wind and solar integration study phase 2," *National Renewable Energy Laboratory, NREL/TP-5500*, vol. 55588, 2013.

[6] D. S. Callaway, "Tapping the energy storage potential in electric loads to deliver load following and regulation, with application to wind energy," *Energy Conversion and Management*, vol. 50, no. 5, pp. 1389–1400, 2009.

[7] H. Hao, A. Kowli, Y. Lin, P. Barooah, and S. Meyn, "Ancillary service for the grid via control of commercial building HVAC systems," in *American Control Conference (ACC), 2013*. IEEE, 2013.

[8] Y. Lin, P. Barooah, and S. P. Meyn, "Low-frequency power-grid ancillary services from commercial building HVAC systems," in *SmartGridComm, 2013 IEEE International Conference on*. IEEE, 2013, pp. 169–174.

[9] S. Meyn, P. Barooah, A. Busic, and J. Ehren, "Ancillary service to the grid from deferrable loads: the case for intelligent pool pumps in florida," in *52nd Conference on Decision and Control*. IEEE, 2013.

[10] US Department of Energy, "Buildings energy data book," http://buildingsdatabook.eren.doe.gov/, 2011.

[11] S. Koch, J. L. Mathieu, and D. S. Callaway, "Modeling and control of aggregated heterogeneous thermostatically controlled loads for ancillary services," in *Proc. PSCC*, 2011, pp. 1–7.

[12] J. L. Mathieu, "Modeling, analysis, and control of demand response resources," Ph.D. dissertation, University of California, Berkeley, 2012.

[13] D. Todd, M. Caufield, B. Helms, A. P. Generating, I. M. Starke, B. Kirby, and J. Kueck, "Providing reliability services through demand response: A preliminary evaluation of the demand response capabilities of Alcoa Inc," *ORNL/TM*, vol. 233, 2008.

[14] M. Maasoumy, J. Ortiz, D. Culler, and A. Sangiovanni-Vincentelli, "Flexibility of commercial building hvac fan as ancillary service for smart grid," *arXiv preprint arXiv:1311.6094*, 2013.

[15] H. Hao, T. Middelkoop, P. Barooah, and S. Meyn, "How demand response from commercial buildings will provide the regulation needs of the grid," in *50th Annual Allerton Conference on Communication, Control and Computing*, October 2012, invited paper.

[16] H. Hao, A. Kowli, Y. Lin, P. Barooah, and S. Meyn, "Ancillary service to the grid through control of fans in commercial building HVAC systems," *IEEE Transactions on Smart Grid*, 2013, under review.

[17] PJM, "PJM manual 12: Balancing operations, rev. 27," December 2012.

[18] "Commercial buildings energy consumption survey (CBECS): Overview of commercial buildings, 2003," Energy information administration, Department of Energy, U.S. Govt., Tech. Rep., December 2008. [Online]. Available: http://www.eia.doe.gov/emeu/cbecs/cbecs2003/overview1.html

[19] Siemens, "APOGEE powers process control language (PPCL) users manual," October 2000. [Online]. Available: http://home.comcast.net/~fredrock/mvc/Siemens_ppcl.pdf

[20] T. Middelkoop, "High-resolution data collection for automated fault diagnostics," in *Automated Diagnostics*, B. L. Capehart and M. Brambley, Eds. Atlanta, GA: Fairmont Press, 2014, in press.

[21] C. Hubner, T. Hansemann, and H. Merz, *Building Automation*, ser. Signals and Communication Technology. Springer Berlin Heidelberg, 2009, pp. 185–273.

[22] L. Ljung, *System Identification: Theory for the User*, 2nd ed. Prentice Hall, 1999.

[23] American Society of Heating, Refrigerating and Air Conditioning Engineers, "ASHRAE Standard 62.1," 2004.

[24] S. Goyal, H. Ingley, and P. Barooah, "Occupancy-based zone climate control for energy efficient buildings: Complexity vs. performance," *Applied Energy*, vol. 106, pp. 209–221, June 2013.

[25] American Society of Heating, Refrigerating and Air Conditioning Engineers, "The ASHRAE handbook fundamentals (SI Edition)," 2005.

[26] PJM, "PJM manual 28: Operating agreement accounting, rev. 62," August 2012.

[27] ——, "PJM manual 11: Energy and ancillary services market operations, rev. 62," December 2013.

[28] ——, "PJM regulation zone preliminary billing data," Jan 2014. [Online]. Available: http://www.pjm.com/markets-and-operations/market-settlements/preliminary-billing-reports/pjm-reg-data.aspx